Supplementary Materials- Large magnetic moment in flexoelectronic silicon at room temperature

Paul C. Lou[1‡], Anand Katailiha[1‡], Ravindra G. Bhardwaj[1‡], Ward P. Beyermann[2], Dominik M. Juraschek[3], and Sandeep Kumar[1,4,*]

[1]Department of Mechanical engineering, University of California, Riverside, CA 92521, USA

[2] Department of Physics and Astronomy, University of California, Riverside, CA 92521, USA

[3] Harvard John A. Paulson School of Engineering and Applied Sciences, Harvard University, Cambridge, MA 02145, USA

[4] Materials Science and Engineering Program, University of California, Riverside, CA 92521, USA

Materials and methods

The devices were made using micro/nano fabrication methods. The sample and electrodes were patterned using photolithography. The device layer Si (wafer resistivity-0.001-0.005 Ω-cm) was then etched using deep reactive ion etching (DRIE). The samples were then made freestanding using the hydrofluoric acid (HF) vapor etch, as shown in Supplementary Figure S1. The HF vapor etched the SiO_2 underneath the patterned sample. Using an optical microscope, the HF vapor etch was stopped once the undercut in the oxide was sufficient to make the sample freestanding. Then, the MgO layer was deposited using an RF magnetron sputtering system. The metal layers (Pt or Py) were deposited using e-beam evaporation. E-beam evaporation was used since it gave a line-of-sight deposition as well as large residual stresses. In the case of the Py layer, we also deposited 1 nm of Pd to protect the Py layer from oxidation.

The ADMR measurement in the Pt/p-Si sample was carried out using delta mode with a Keithley 6221 current source and a 2182A nanovoltmeter. The delta mode utilized the current reversal technique to cancel out any constant thermoelectric offsets, which was essential to minimize the thermal transport effects. The magnitude of the current used for measurement is 100 μA.

All the other measurements were carried out using an AC lock-in technique in the low frequency regime (5-37 Hz). The low frequency measurement lead to a quasi-static response and a time-dependent response is not recorded.

Supplementary Figures

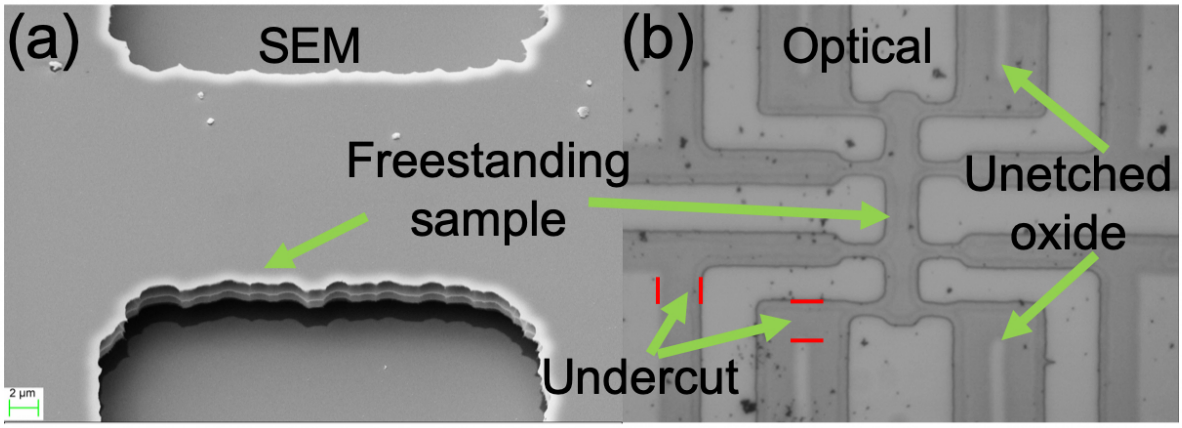

Supplementary Figure S1. (a) A scanning electron micrograph showing the freestanding nature of the sample (reflection). The oxide layer underneath the sample area is etched using an HF vapor etch. (b) An optical micrograph showing the etch contrast in the freestanding sample area and undercut at electrodes and connecting arms. The undercut in the oxide layer is essential for making the sample freestanding.

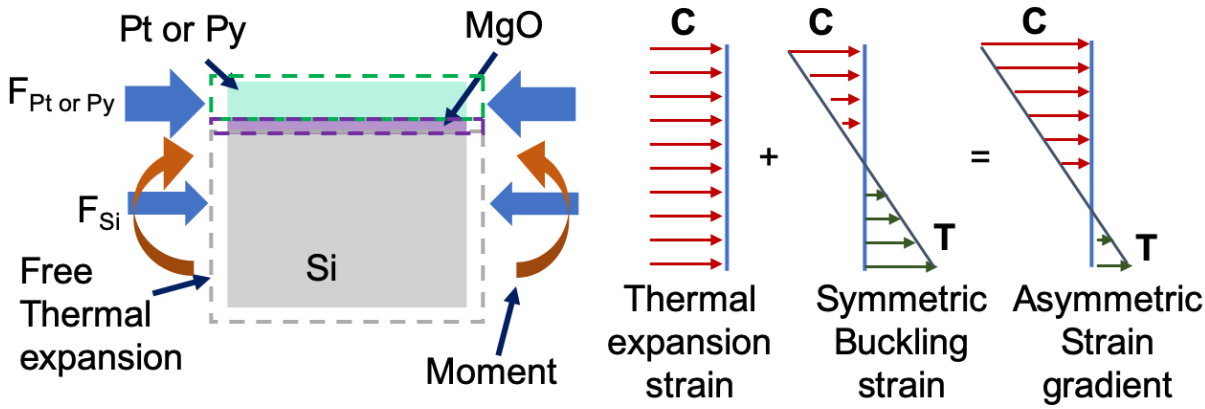

Supplementary Figure S2. A schematic showing the origin of the asymmetric strain gradient, which is the underlying cause of asymmetric electronic charge separation. The thermal expansion gives rise to different forces in the Si and Pt (Py) layers. The displacement $(u(z))$ and strain $\left(\frac{\partial u}{\partial x}(z)\right)$ fields through the thickness are continuous

across the interface but stress field is discontinuous. The strain field will be continuous across the length except at boundaries and will only be a function of boundary condition for the freestanding thin films structure. The C and T represent compression and tension, respectively.

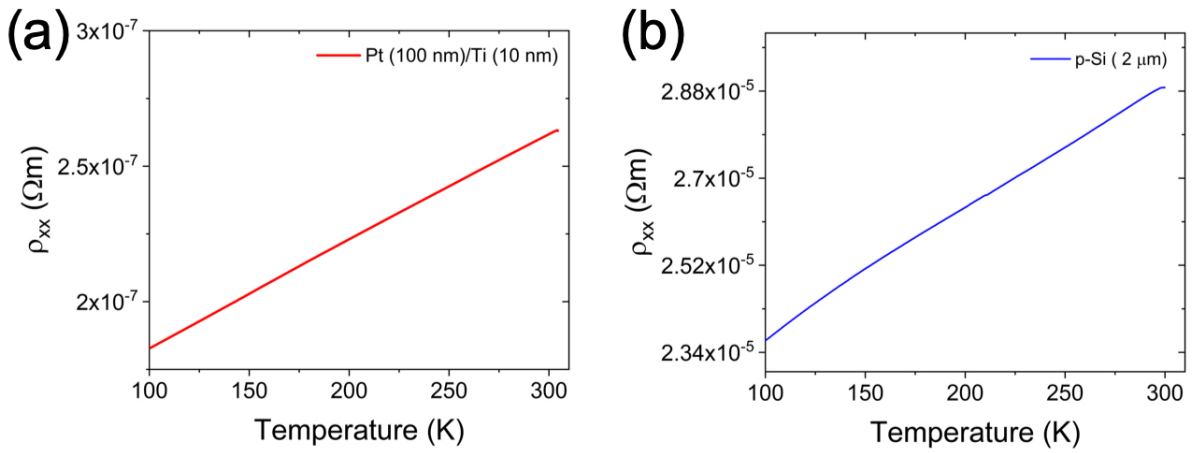

Supplementary Figure S3. The resistivity as a function of temperature between 300 K and 10 K for (a) Pt (100 nm)/Ti (10 nm) and (b) p-Si (2 μm) samples. In case of Pt, the sample thickness of 100 nm was chosen to reduce/eliminate the contribution of Ti (10 nm) adhesion layer. No Ti adhesion layer was needed the Pt/p-Si sample since there was no post processing of the sample. Whereas Pt/Ti sample was deposited using lift-off lithography, where extended solvent treatment was needed. The p-Si sample has significantly higher resistivity than the estimated resistivity of p-Si layer in Pt/p-Si composite sample, which is attributed to the flexoelectric charge separation. The resistivity of the p-Si layer in Pt/p-Si composite sample was estimated by assuming constant Pt resistivity.

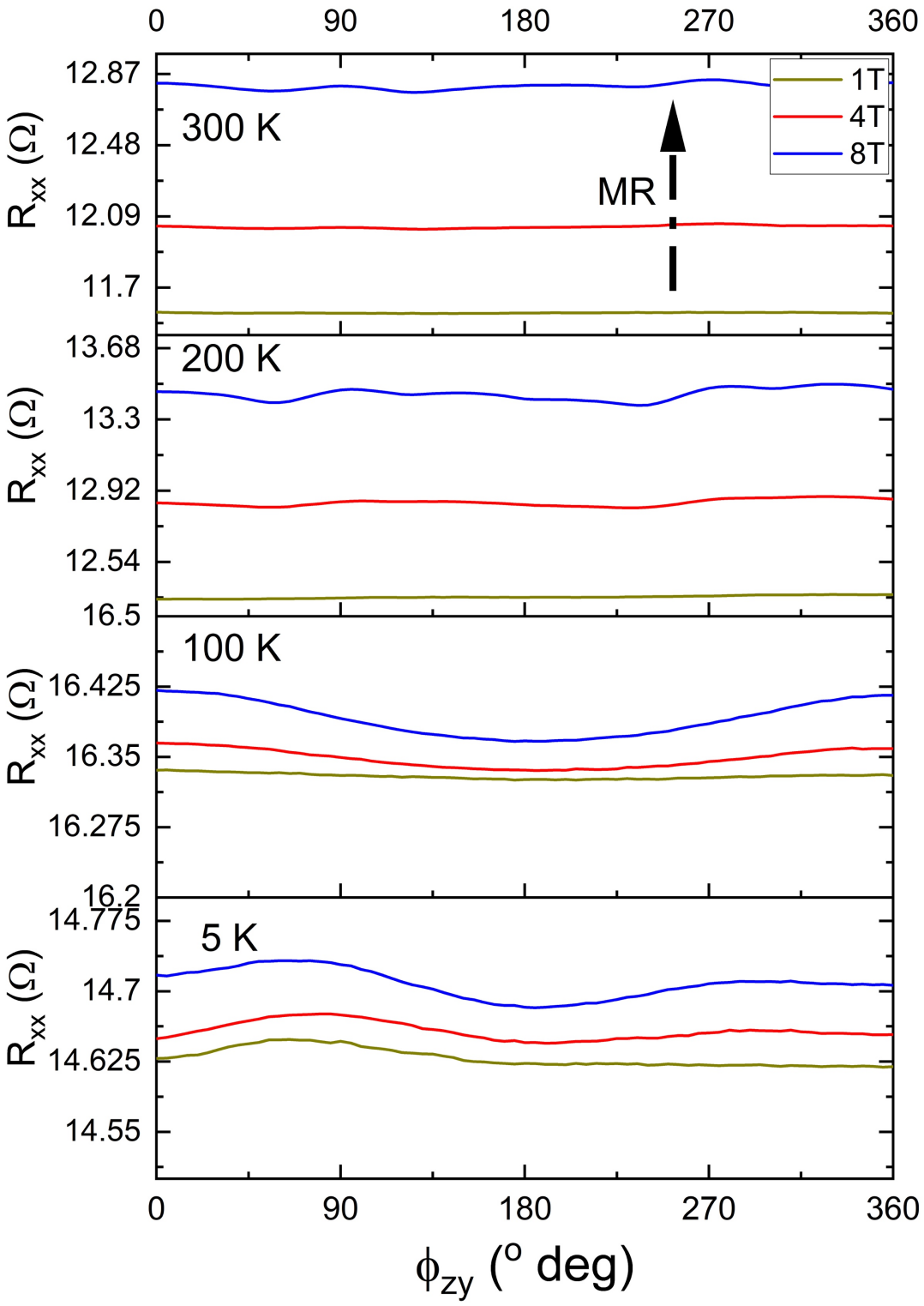

Supplementary Figure S4. The angle-dependent longitudinal resistance as a function of constant magnetic field of 1 T, 4 T and 8 T at 300 K, 200 K, 100 K and 5 K.

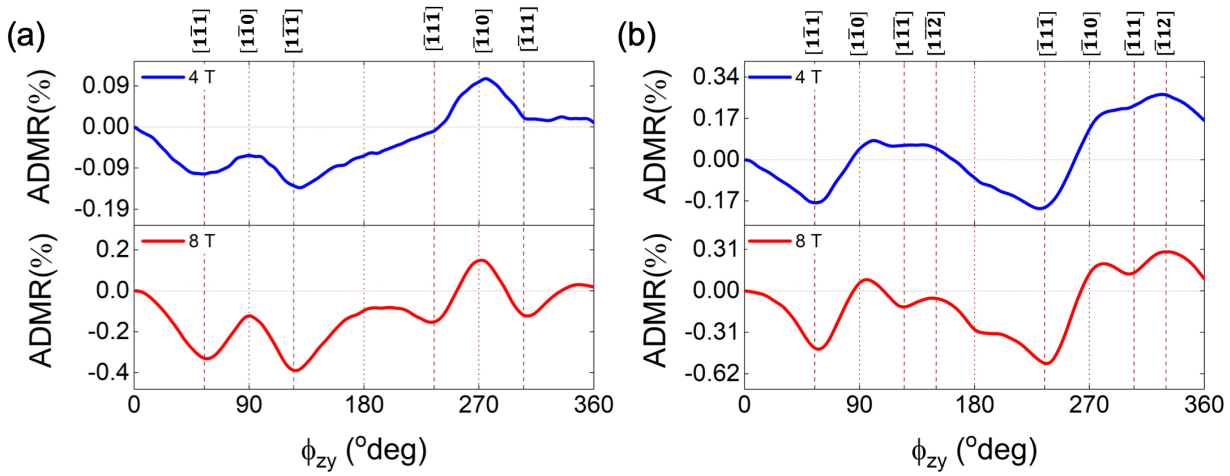

Supplementary Figure S5. The ADMR response at 300 K and 200 K showing the crystallographic direction-dependent anisotropy.

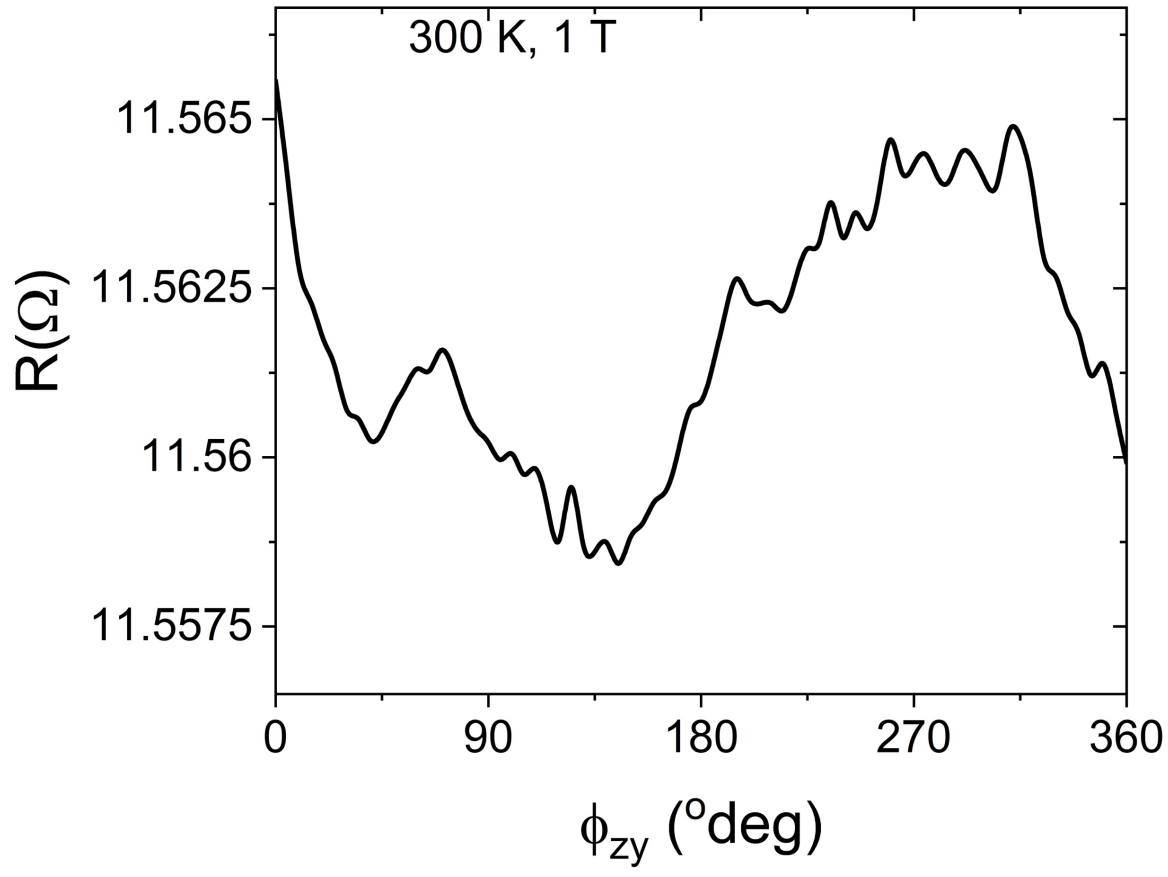

Supplementary Figure S6. The angle-dependent longitudinal resistance at 300 K and 1 T magnetic field showing weak direction dependent behavior.

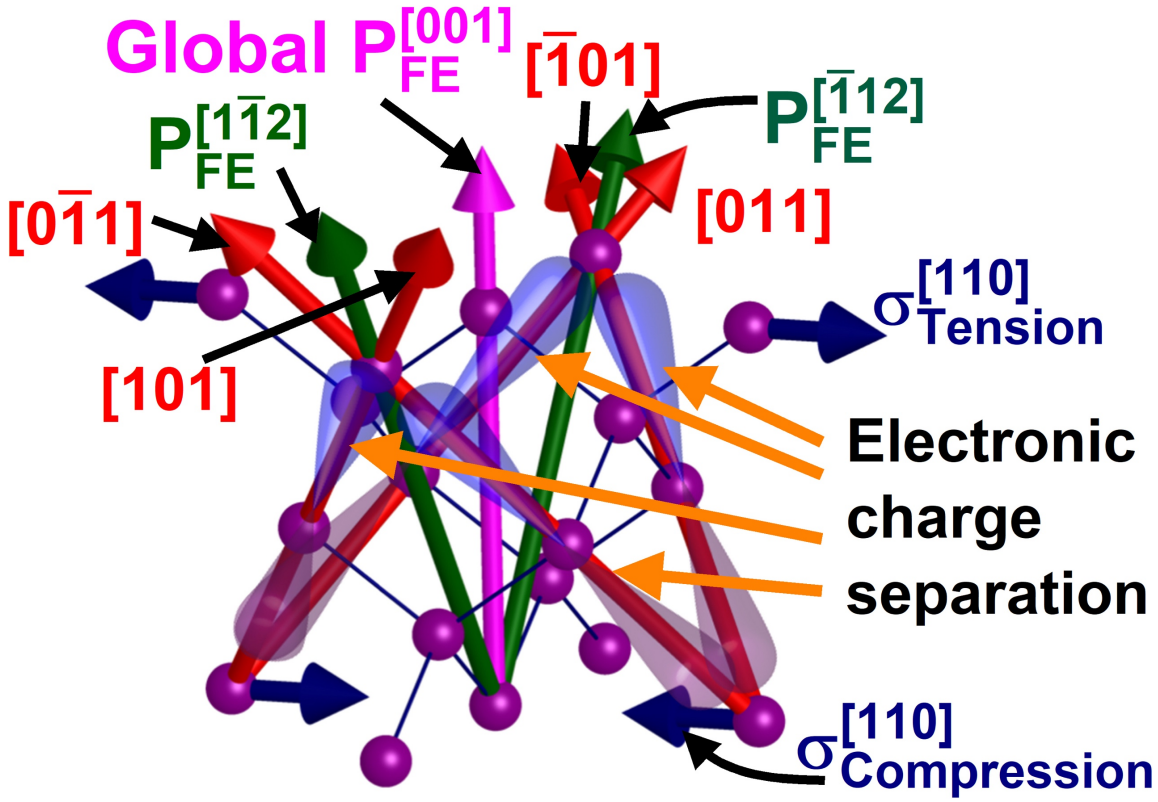

Supplementary Figure S7. A schematic showing the electronic charge separation along four $< 110 >$ directions and, as a consequence, local flexoelectronic polarization was along $[1\bar{1}\bar{2}]$ and $[\bar{1}12]$. The global flexoelectronic polarization was $[001]$ and parallel to the strain gradient direction.

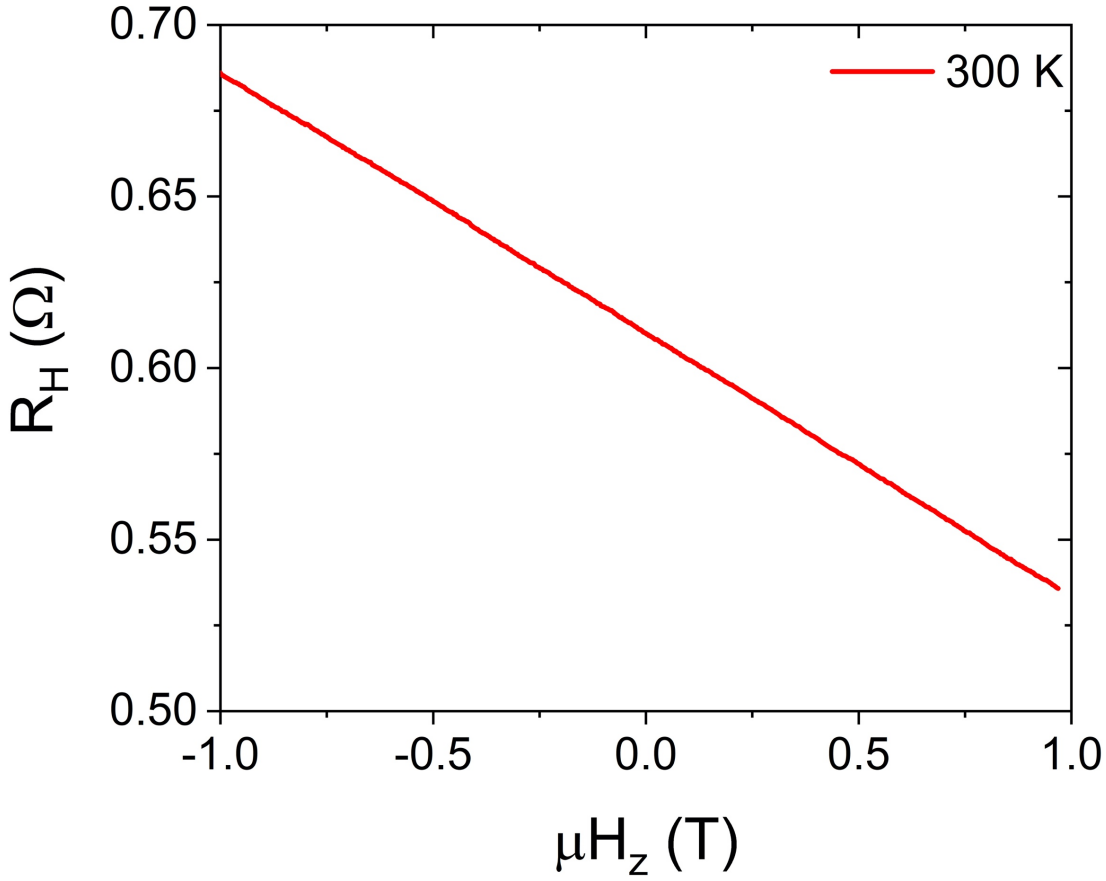

Supplementary Figure S8. The Hall effect measurement on an MgO (2 nm)/p-Si (2 μm) sample using 2 mA of current. In spite of p-doped Si, the Hall resistance showed a negative slope corresponding to the electrons being the charge carrier. This behavior might arise due to charge separation from the flexoelectronic effect.

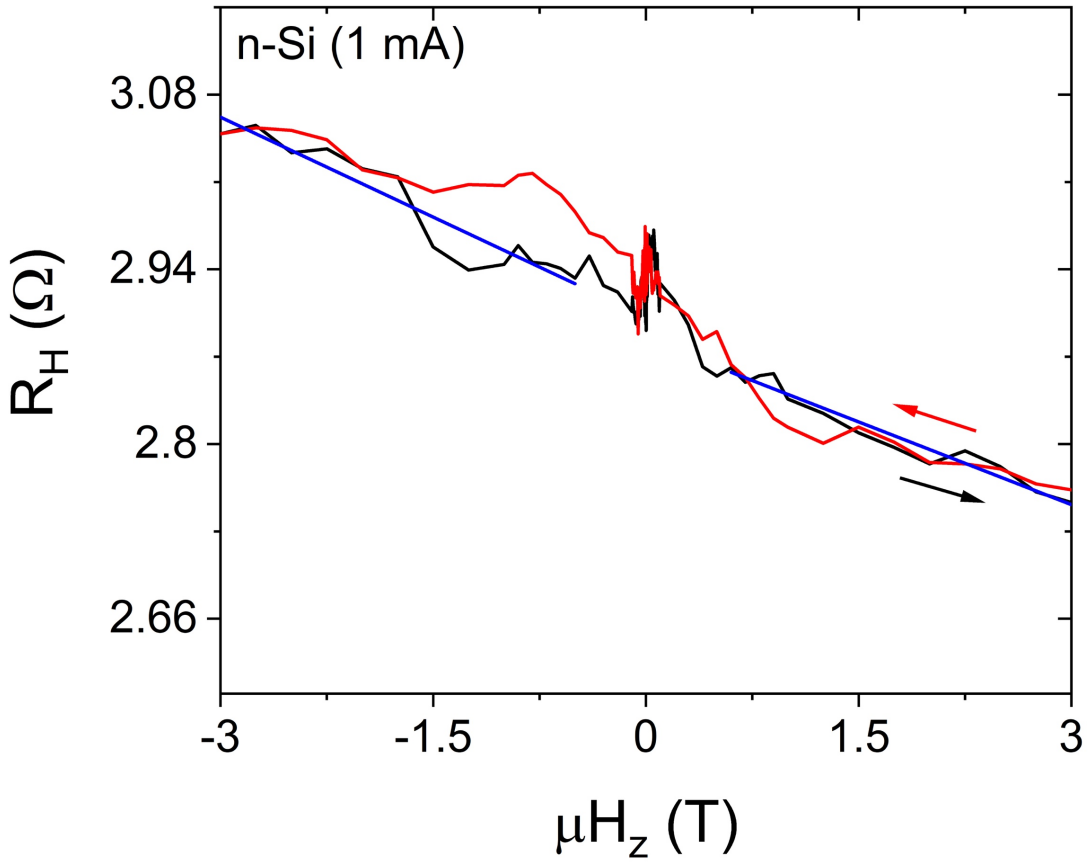

Supplementary Figure S9. The Hall effect measurement on an MgO (2 nm)/n-Si (2 μm) sample using 1 mA of current. As compared to the measurement at 5 mA shown in main text, this measurement did not show AHE behavior explicitly. We attribute this behavior to a smaller strain gradient. The charge carrier concentration is estimated to be ~5.9×10^{19} cm^{-3} at 1 mA current in this measurement. Assuming a saturation magnetic field of 0.7 T from Figure 4 (d), we estimate the maximum R_{AHE} to be -8.85±6.8 mΩ as compared to -34.13 mΩ at 5 mA. However, there is no clear switching field in this measurement. The blue lines are line fits.